Available online at www.sciencedirect.com
SCIENCE DIRECT®
Journal of Solid State Chemistry 177 (2004) 3954–3962
JOURNAL OF SOLID STATE CHEMISTRY
www.elsevier.com/locate/jssc

Synthesis and characterization of layered double hydroxides (LDH) intercalated with non-steroidal anti-inflammatory drugs (NSAID)

Margarita del Arco[a], Sonia Gutiérrez[a], Cristina Martín[a], Vicente Rives[a,*], Joao Rocha[b]

[a]*Departamento de Química Inorgánica, Universidad de Salamanca, Salamanca, Spain*
[b]*Department of Chemistry, CICECO, University of Aveiro, 3810-193 Aveiro, Portugal*

Received 8 July 2004; received in revised form 26 July 2004; accepted 2 August 2004
Available online 18 September 2004

Abstract

Layered double hydroxides (LDHs) with the hydrotalcite type structure and a Mg:Al ratio of two have been prepared, with salicylate or naproxen in the interlayer. Two synthetic routes have been used: reconstruction from a mildly calcined hydrotalcite-CO_3 precursor, and a coprecipitation method with chlorides of the metals. The solids have been characterized using several physicochemical techniques, i.e., powder X-ray diffraction, FTIR and ^{13}C CP/MAS NMR spectroscopies and thermal analysis (thermogravimetric and differential thermal analyses). The gallery height determined is in all cases larger than the size of the drug, 11.5 Å for salicylate and 15.8 and 16.6 Å for naproxen, depending on the specific synthesis route followed. Experimental data suggest the anion molecules form a tilted bilayer, with the carboxylate groups pointing towards the brucite-like layers. The solids are stable up to 230 °C and their evolution from 350 °C upwards is very similar to that observed for a carbonate-containing hydrotalcite, forming mostly amorphous solids with a large specific surface area.

Keywords: Hydrotalcite; Layered double hydroxides; Non-steroidal drugs; Intercalation compounds

1. Introduction

Different inclusion compounds are currently being used in pharmaceutical formulations to avoid the adverse physicochemical properties of some drugs, such as bad odor, low solubility, volatility, decomposition under irradiation, water, oxygen, etc. β-cyclodextrins are used for these purpouses, because of their ability as biocompatible hosts for compounds with pharmaceutical or biological interest. Layered inorganic compounds, such as kaolinite, bentonite or montmorillonite, are also used in some cases as excipients or adsorbents for several drugs.

The so-called layered double hydroxides (LDHs), also known as anionic clays, are attracting a lot of interest in recent years because of their wide applications, such as catalysts and catalyst precursors, adsorbents, electrochemicals, hosts for nanoscale reactions, etc. The LDH structure consists of brucite—$Mg(OH)_2$—layers where a partial Mg^{2+}/Al^{3+} substitution has taken place, thus requiring interlayer anions to balance the positive charge of the layers. The general formula is $[M^{2+}_{1-x}M^{3+}_{x}(OH)_2][A_{x/n}\cdot mH_2O]$, where $x = M^{3+}/(M^{2+}+M^{3+})$ and n is the formal charge of the anion. As it can be concluded from the formula, the formal positive charge of the layer depends on the M^{2+}/M^{3+} ratio. Although the commonest anion is carbonate, many LDHs have been synthesized with different anions, both organic and inorganic, such as halides, silicates, polyoxometalates, anionic coordination compounds, carboxylates, etc. [1–9]; among the organic anions, intercalation of benzoate and terephtalate inclusion has been also widely studied [10–18].

The ability of these compounds to exchange the interlayer anion has been clearly proven in the literature

*Corresponding author. Fax +34-923-29-45-74.
E-mail address: vrives@usal.es (V. Rives).

0022-4596/$ - see front matter © 2004 Elsevier Inc. All rights reserved.
doi:10.1016/j.jssc.2004.08.006

and, thus, they may be used as biocompatible hosts for several drugs, such as NSAID (non-steroidal anti-inflammatory drugs), widely used in rheumatism treatment, which very often show adverse secondary effects, such as gastric and duodenal ulcers formation; most of these drugs are aromatic organic compounds with easily ionizable carboxylic groups, and so they could be hopefully intercalated in the interlayer space of hydrotalcites (in the anionic form) to produce a sustained release formulation.

The applications of the $MgAl–CO_3$ hydrotalcite (that is, with Mg^{2+} and Al^{3+} in the brucite-like layers, and carbonate in the interlayer) in Medicine and Pharmacy have been almost exclusively restricted to its role as antacid or anti-pepsinic, as it is the active component of commercial drugs such as Almax®, Bemolan®, Talcid®, etc. [19–21]. It is also used in dentifrices, deodorants, and as excipient or intestinal phosphate adsorbents [22,23]. However, the literature concerning the use of hydrotalcite materials as drug hosts is very scarce; most of the data published concern patents or proceedings [24–29], and the intercalation of ibuprofen, dichlofenac, indometacin, tolmentin, etc., in MgAl–Cl hydrotalcites by anion exchange has been described, obtaining materials containing 22–48% (w/w) of the drug. Ambrogi et al. [30] have recently reported the intercalation of different NSAIDs, finding that encapsulation of these drug molecules in hydrotalcite improves the solubility of the drug; this finding is very important because solubility plays a key role in liberation, absorption and bioavailability of the drug.

In this paper we report on the incorporation of two NSAID, salicylic acid and naproxen, in MgAl hydrotalcites, following two synthetic routes and diferent experimental conditions (e.g., pH, temperature and reaction time). The aim of the work is to intercalate the organic molecules in the interlayer space of the LDH in order to improve their solubility in an acidic medium, as well as lowering the direct gastrolesivity of the anti-inflammatory drugs. Full characterization of the solids prepared has been achieved using powder X-ray diffraction, FTIR and ^{13}C cross-polarization (CP) magic-angle spinning (MAS) NMR spectroscopies, adsorption of nitrogen at $-196\,^{\circ}C$ for surface area assessment and thermal analysis to determine their thermal stability.

2. Experimental

The Mg_2Al–NSAID samples have been prepared following two different routes: reconstruction from a calcined $Mg_2Al–CO_3$ and direct synthesis by coprecipitation from Mg and Al chlorides.

2.1. Reconstruction

A $Mg_2Al–CO_3$ LDH (prepared by conventional coprecipitation [1] and with a basal spacing of 7.7 Å) sample was calcined at 500 °C for 2 h under a nitrogen flow (ca. 30 ml/min). A solution containing 1.5 g of salicylic acid in 75 ml of water, at pH = 4 attained by addition of 2 M KOH, was added to 2 g of calcined $Mg_2Al–CO_3$ LDH. The final mixture at pH = 9 (by adding 2 M KOH) was magnetically stirred at room temperature for 6 h while bubbling nitrogen. The solid was washed several times with decarbonated water and was dried in a vacuum desiccator, leading to sample named SalR.

The sample with naproxen was prepared by adding 1 g of $Mg_2Al–CO_3$ hydrotalcite calcined to a solution prepared dissolving 1.34 g naproxen and 0.32 g KOH in 75 ml decarbonated water. Also in this case the pH was adjusted to a value of 9 and the suspension was stirred for 6 h at room temperature, while bubbling nitrogen. The solid was centrifugued, washed and dried in a vacuum desiccator, leading to sample NapR.

2.2. Coprecipitation

A portion of 50 ml of an aqueous solution containing 11.4 g $MgCl_2 \cdot 6H_2O$ and 6.8 g $AlCl_3 \cdot 6H_2O$ was added to 75 ml of an aqueous solution containing 7.7 g salicylic acid in decarbonated water neutralized with 2 M KOH. The pH was raised to a value of 9 by addition of 2 M KOH and the mixture was magnetically stirred at room temperature for 16 h while bubbling nitrogen. The solid was filtered, washed and dried in a vacuum desiccator; the sample was named as SalC.

Sample NapC was obtained by slowly adding a solution containing 4.4 g $MgCl_2 \cdot 6H_2O$ and 2.6 g $AlCl_3 \cdot 6H_2O$ in 50 mL decarbonated water, to another formed by 2.3 g naproxen and 0.6 g KOH dissolved in 75 mL decarbonated water. Other steps were as for sample SalC.

All syntheses with salicylate were carried out without direct light to avoid decomposition of salicylic acid.

In all cases, the methods were modified using different stirring times (from 3 to 16 h) in order to increase the crystallinity of the product. The quality of the solid did not change after 6 h following the methods of reconstruction; however, longer reaction times were needed for the coprecipitation method. No improvement was observed when the reaction temperature was raised to 50 or 100 °C, but a partial decomposition of salicylic acid was observed. Also pH was varied between 6.5 and 10, the better yields being obtained at pH = 9. When the Mg/Al molar ratio was increased to 3 or 4 no incorporation of the organic molecule was observed.

2.3. Experimental techniques

Elemental chemical analyses were carried out in Servicio General de Análisis Químico Aplicado (University of Salamanca, Spain); atomic absorption in a Mark 2 ELL-240 instrument was used for Mg and Al analysis after dissolving the samples in nitric acid, while C was analyzed in an Elemental Leco, model CHNS 932 analyzer. Chloride was determined gravimetrically [31].

Powder X-ray diffraction diagrams (PXRD) were collected on a Siemens D-500 using Cu$K\alpha$ radiation ($\lambda = 1.54050$ Å) and quartz as an external standard.

Fourier Transform Infrared spectra (FTIR) were collected in a Perkin–Elmer FT-1730 instrument using the KBr pellet technique; 100 scans were averaged to improve the signal-to-noise ratio, at a nominal resolution of $4\,cm^{-1}$.

Specific surface area measurements were carried out in a Micromeritics Flowsorb II 2300 instrument after degassing in situ the samples at 150 °C.

Differential thermal analyses (DTA) and thermogravimetric analyses (TGA) were measured on DTA7 and TG7 instruments, respectively, from Perkin–Elmer. The analyses were carried out in flowing (30 ml/min) oxygen from L'Air Liquide (Spain).

The ^{13}C CP/MAS NMR spectra were recorded at 100.62 MHz in a Bruker Avance 400 spectrometer using 4 μs ^{1}H 90° pulses, a contact time of 2 ms, a 5 s recycle delay and a 9 kHz spinning rate. Chemical shifts are given in ppm from TMS.

In order to analyze the thermal stability of the solids and to identify the phases formed, the solids obtained upon calcination at temperatures ranging from 100 to 800 °C were also characterized.

3. Results

3.1. Element chemical analysis

Element chemical analysis for Mg, Al, and C for the samples prepared are included in Table 1. The molar Mg/Al ratio was in all cases reasonably close to the expected value of 2, the value in the precursor hydrotalcites used in the reconstruction (samples SalR and NapR) and with the ratio in the precursor chlorides used in the coprecipitation method (samples SalC and NapC). The amount of drug incorporated, as determined from the carbon content, depends on the specific synthetic route followed. The Al/NSAID ratio should be 1.0 if salicylate or naproxen is the only interlayer anion, balancing the positive charge of the Al^{3+} cations in excess to that of the Mg^{2+} cations. The value measured is, however, larger than the expected one in all cases, especially for sample NapR, suggesting that other anions, such as carbonate, chloride or hydroxyl, in addition to salicylate or naproxen, exist in the interlayer, balancing the positive charge of the layers. Minor amounts of chloride have been found in samples prepared by coprecipitation (0.05% in SalC and 0.03% in NapC), probably by contamination of the precursor salts.

3.2. Specific surface area

The specific surface areas of the samples and of the solids obtained upon calcination at increasing temperatures are given in Tables 1 and 2, respectively.

The specific area of samples SalC and SalR are $7\,m^2g^{-1}$ and the value is practically the same after calcination of the samples at 200 °C. However, as the calcination temperature is increased above 200 °C, the specific surface area increases sharply.

Table 2
Change in the specific surface area of the samples upon calcination at increasing temperatures

Calcination temperature (°C)	SalC	NapC
Original	7	20
300	54	76
500	138	95
700	130	n.m.
800	93	212

n.m. = not measured.

Table 1
Element chemical analysis data, specific surface areas, and lattice parameters of the Mg_2Al–NSAID samples prepared

Sample	%Mg[a]	%Al[a]	%C[a]	Mg/Al[b]	Al/NSAID[b]	S_{BET}[c]	c[d]	a[d]
SalR	14.35	8.34	20.88	1.91	1.2	7	48.9	3.05
SalC	13.47	7.58	17.56	1.97	1.3	7	48.9	3.03
NapR	12.50	6.36	28.16	2.18	1.4	20	64.1	3.04
NapC	12.75	6.93	34.23	2.04	1.2	19	61.9	3.03

[a]Weight percentage.
[b]Molar ratio.
[c]m^2/g.
[d]Å.

The values determined for samples NapC and NapR are 20 $m^2 g^{-1}$ and correspond to ca. three times the value measured for the salicylate samples. The value does not change when the samples are calcined below 200 °C. As with the salicylate samples, due to the organic nature of the interlayer anion and the formation of essentially amorphous samples upon calcination (see below) a strong surface area development is observed upon calcination above this temperature, Table 2. Such a surface area development has been previously reported for calcined hydrotalcites containing vaporizable anions in the interlayer, i.e., carbonate, nitrate, organic anions, etc., which form gases or vapors upon calcination (CO_2, NO_2, H_2O, etc.) [32,33] which escape through the basal planes of the crystals, forming fine tunnels and chimneys which are responsible for the surface area increase.

3.3. Powder X-ray diffraction

The PXRD diagrams for the samples with salicylate and naproxen are included in Fig. 1. The diagrams of the salicylate-containing samples, Fig. 1a, correspond to well crystallized solids with the hydrotalcite-like structure, and no diffraction line due to the free drug has been recorded in any case. Moreover, the first peak recorded at low diffraction angle corresponds to a basal spacing larger than that corresponding to a hydrotalcite with carbonate in the interlayer (7.7 Å), suggesting the drug molecules have been intercalated between the brucite-like layers. The basal spacing recorded was 16.3 Å for samples SalR and SalC. Harmonic diffraction lines are also recorded at the corresponding spacings 8.14 and 5.4 Å. Some of these peaks, however, are unusually broad. According to Jones et al. [15] development of broad, asymmetric peaks in the diagrams of hydrotalcites containing interlayer benzoate is due to a deffective stacking of the layers, as the crystals mainly grow in a given direction, parallel to the brucite-like layers.

For the samples with naproxen, Fig. 1b, the basal spacings recorded were 21.37 and 20.63 Å, respectively, for samples NapR and NapC. The values are rather similar and suggest the drug has been incorporated in the interlayer of the solids. In addition, the diffraction lines due to planes (006) and (009) are recorded at 10.3 and 6.8 Å for sample NapC and at 10.67 and 7.13 Å for sample NapR.

The lattice parameters of the samples, calculated from the positions of the maxima due to reflection by planes (003) for parameter *c*, and planes (110) for parameter *a*, are included in Table 1. The *c* parameters for samples hydrotalcite–naproxen are larger than those observed for the hydrotalcite–salicylate samples. This fact can be related to the larger size of naproxen, and suggests that the molecules are not oriented with their plane parallel to the brucite-like layers, but somewhat upwards or

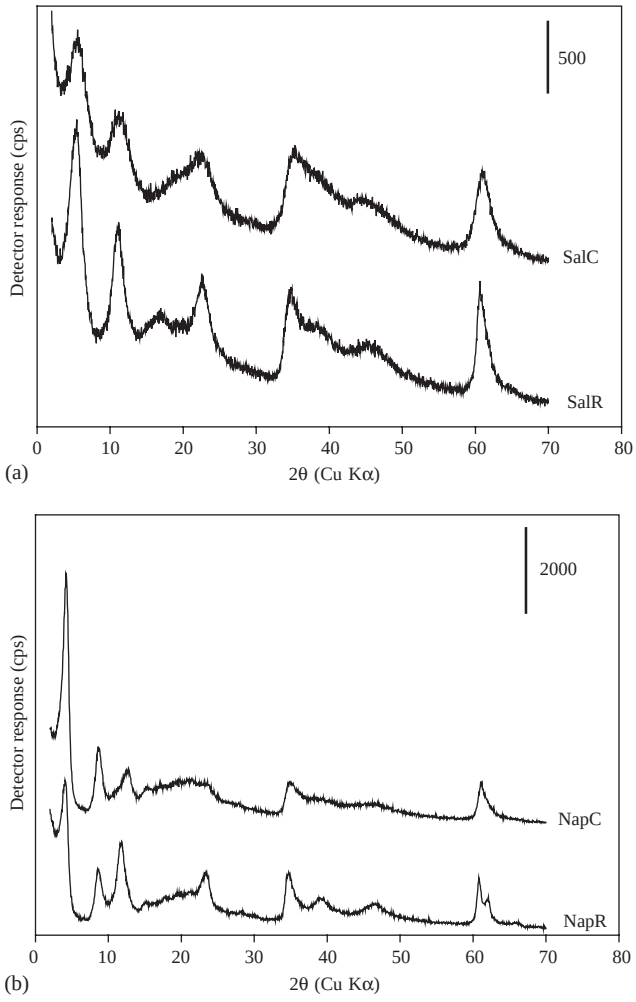

Fig. 1. Powder X-ray diffraction diagrams for the (a) Mg_2Al–salicylate and (b) Mg_2Al–naproxen samples (the diagrams have been vertically displaced).

tilted. However, the *a* parameters are almost identical for both series of samples, as a consequence of the same cations existing in the layers in almost the same molar ratio (see Table 1); the *a* values are in the range generally reported for LDHs with Mg^{2+} and Al^{3+} in the brucite-like layers [34]. The presence of a given amount of the carbonate hydrotalcite cannot be completely excluded, because of the ubicuous presence of CO_2 (despite a nitrogen atmosphere was used in all cases) and some of the diffraction maxima of the carbonate hydrotalcite are coincident with strong peaks of the compounds prepared. This could be especially true for sample NapR, which shows rather broad diffraction maxima. Also for this sample, the element chemical analyses suggest the presence of a carbonate-hydrotalcite.

3.4. FTIR spectroscopy

The FTIR spectra of the samples are included in Fig. 2. The presence of several functional groups in the

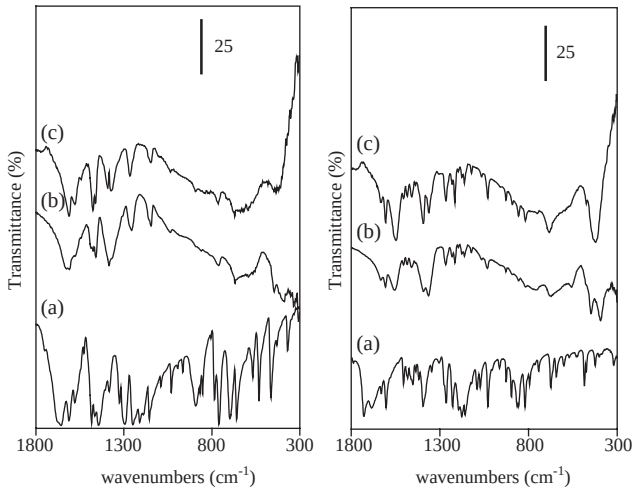

Fig. 2. FTIR spectra of: left (a) salicylic acid, (b) sample SalR and (c) sample SalC; right (a) naproxen, (b) sample NapR and (c) sample NapC.

salicylic acid gives rise to a spectrum with many absorption bands. In addition to bands at high wave number values, due to ν(OH) and ν(=C–H) moieties, a band is recorded at 1658 cm^{-1}, due to mode ν(C=O) of the acid group; the abnormally low value for the position of this band is due to intramolecular hydrogen bonds. The bands due to ν(C–C) of the aromatic ring are recorded at 1613, 1579, 1484, and 1467 cm^{-1}; those due to modes ν(C–O) and δ(O–H) of the acid and alcohol functions are recorded at 1441, 1292, 1240, and 1290 cm^{-1}, while in-plane and out-of-plane δ(CH) bands are recorded below 1000 cm^{-1} [35].

As the X-ray diffraction diagrams for these samples did not show any maximum due to the free drug, the bands recorded in the FTIR spectra of these samples should be exclusively due to the drug-intercalated compounds. However, the drug is intercalated in the anionic form, and consequently the band due to mode ν(CO) of the acid has vanished, while other bands, due to $\nu_{as}(COO^-)$ and $\nu_s(COO^-)$ modes of the carboxylate group, develop at 1550 and 1386 cm^{-1}, respectively. The positions of these bands are close to those reported for hydrotalcites containing intercalated benzoate with different electric layer charges [14]. A new band is recorded at 1364 cm^{-1}, with different widths from one sample to another, which may correspond to mode ν_3 of carbonate units, though the contaminating carbonate hydrotalcite has been not detected by PXRD. The other bands recorded are very similar, with respect to their positions and relative intensities, to those recorded in the spectrum of the free drug. Additionally, bands are recorded in the low wave number region at 560 and 393 cm^{-1}, due to Mg/Al–OH translation modes [36].

The FTIR spectrum of naproxen (Fig. 2) shows also a large number of bands, due to the different functional groups existing in this molecule. The most representative bands are recorded in the following positions: the bands at 1729 and 1686 cm^{-1} are due to mode ν(C=O) of the carboxylic group, free or hydrogen bonded; several bands in the 1631–1459 cm^{-1} range are due to ν(C–C) modes of the aromatic groups. The band due to mode $\delta(CH_3)$ is recorded at 1398 cm^{-1}, and those due to modes ν(CO) and ν(C–O–C) of the ether group are recorded between 1265 and 1162 cm^{-1}. Finally, the bands due to δ(CH) modes are recorded below 1000 cm^{-1} [35].

The spectra recorded after incorporation of the drug are very similar. Because of the ionization of the acid group, the bands detected for free naproxen at 1729 and 1686 cm^{-1} disappear, and a new band at 1547 cm^{-1} is recorded, which is due to the $\nu_{as}(COO^-)$ mode, together with another band at 1364 cm^{-1}, due to the symmetric vibration, $\nu_s(COO^-)$; the band originated by the $\delta(CH_3)$ mode is recorded at 1392 cm^{-1}. A band at 1364 cm^{-1}, due to mode ν_3 of the carbonate anion, is also recorded; this band is broader for sample NapR than for the sample NapC. Other bands are recorded in positions very close to those for the free naproxen. Additionally, bands due to Mg/Al–OH translational modes are recorded [36].

3.5. ^{13}C CP/MAS NMR spectroscopy

The spectra of the drug and hydrotalcite–salycilate samples prepared are given in Fig. 3. The most representative shifts and their attribution are summarized in Table 3. The carboxylic group resonance of the free drug is observed at 175.8 ppm, while that for the alcohol group is recorded at 161.6 ppm. Similar chemical shifts are observed for the two samples prepared. Weak signals are recorded at ca. 170 and 165.1 ppm for both samples. These two resonances, absent from the spectrum of the free drug, are attributed to carbonate and bicarbonate species, respectively [37]; as mentioned above, the presence of carbonte hydrotalcite could not be absolutely excluded from the PXRD data.

The spectra of the naproxen and the two hydrotalcite–naproxen samples prepared are given in Fig. 4.

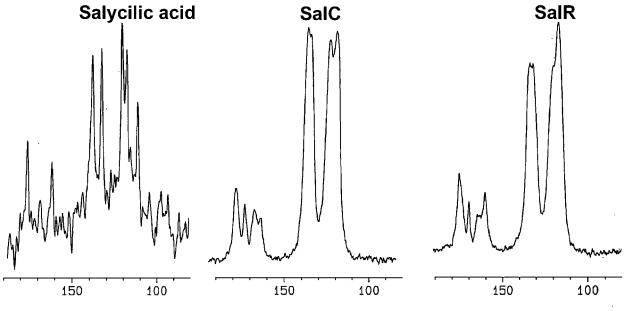

Fig. 3. ^{13}C CP/MAS NMR spectra of salicylic acid and of the Mg_2Al–salicylate samples.

Table 3
^{13}C CP/MAS NMR resonances of Mg_2Al–salicylate samples

Attribution	Salycilic acid	SalR	SalC
–COOH; $–COO^-$	175.8	175.2	175.2
CO_3^{2-}		169.9	169.9
HCO_3^-		165.1	164.4
C–OH	161.6	160.6	160.6
C or CH ring	138.0–111.4	134.9–117.2	134.1–117.2

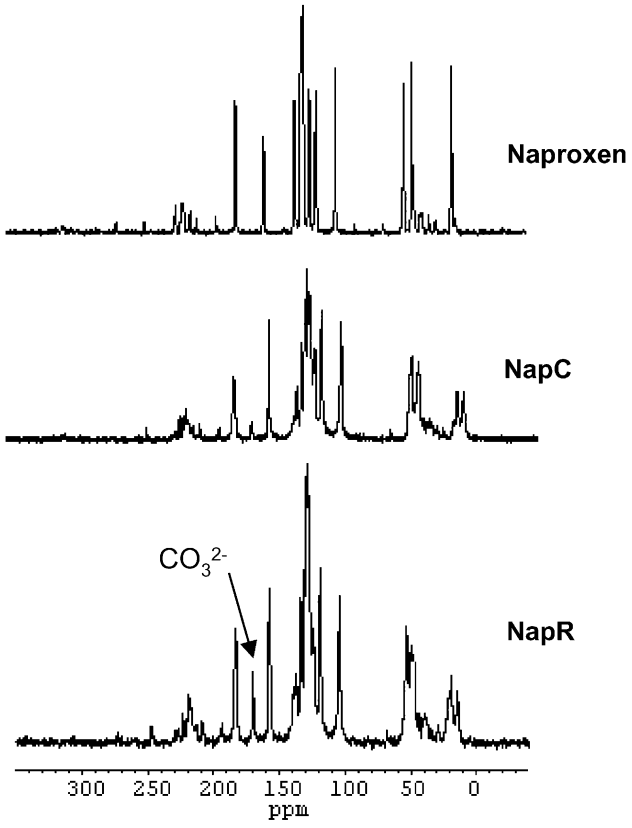

Fig. 4. ^{13}C CP/MAS NMR spectra of naproxen and of the Mg_2Al–naproxen samples.

Table 4
Chemical shifts in the CP/MAS ^{13}C NMR spectra of the Mg_2Al–naproxen samples

Ascription	Naproxen	NapR	NapC
–COOH; $–COO^-$	178.2	183.0	183.0
CO_3^{2-}		169.8	169.8[a]
(C–O) ether	156.6	157.6	157.5
C, CH ring	144.2–104.5	139.1–104.5	140–104.3
CH_3(ether)	55.4	53.5	52.4
C (close to COOH)	44.4	44.3	47.5
CH_3 (close to COOH)	18.7	19.1	18.9

[a]Extremely weak.

The most representative chemical shifts and their attribution are summarized in Table 4. The values for the hydrotalcite samples and free naproxen are very similar, the small differences observed being probably due to the interaction of the anionic form of naproxen with the brucite-like layers.

The ^{13}C CP/MAS NMR spectrum of sample NapR shows, in addition, a signal at 170 ppm, which has been also observed in the MgAl–salicylate samples, and is ascribed to Mg_2Al–CO_3 hydrotalcite contaminating these samples. This signal is almost invisible in the spectrum of sample NapC.

3.6. Thermal analyses

To complete the characterization study, TG and DTA have been applied to determine the high temperature thermal stability of the samples prepared. The diagrams, recorded in air, are very similar for the two samples prepared with each drug. The diagrams for samples SalC and NapC are included in Fig. 5. A broad endothermic effect is recorded at ca. 100 °C in the DTA diagram of sample SalC, which should correspond to removal of interlayer water (gases evolved during decomposition were not analyzed). An intense exothermic peak, which exact position is sample-dependent, is recorded between 385 and 400 °C and is due to combustion of the drug, with CO_2 and water vapor evolution. Such a process is completed at ca. 600 °C, although a small weight loss is observed up to 800 °C. Dehydroxylation of the layers usually takes place between 300 and 500 °C, but the corresponding endothermic peak is probably cancelled by the strong exothermic effect due to combustion of the drug.

The TG curve shows two weight losses, the first one coinciding with the endothermic effect generally related to removal of interlayer water molecules, and the second one due to dehydroxylation and combustion of the drug molecule. The first weight loss amounts 16.08 and 20% of the initial sample weight, respectively, for samples SalR and SalC.

In addition to the TG and DTA studies, we have applied other characterization techniques to identify the phases existing after calcination the samples at increasing temperatures. The PXRD diagrams of the samples calcined at 200 °C are similar to those for the uncalcined sample, although the diffraction lines are broadened and

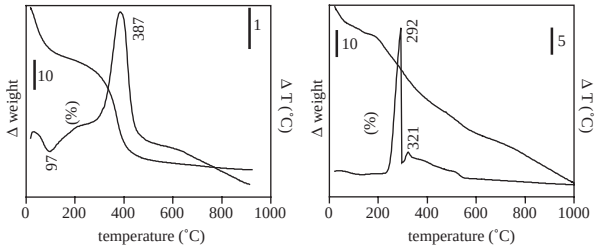

Fig. 5. DTA/TG diagrams of (left) sample SalC, and (right) sample NapC.

those due to diffraction by basal planes are slightly shifted to lower d values, probably because of water removal and an increase in the anion-layer electrostatic interactions. The lines due to the layered system vanish at 300 °C, and the aspect of the diagram resembles that of an amorphous material. These changes are in agreement with the sharp development of the specific surface area (Table 2) from 7 to 54 m^2/g upon calcination at 300 °C. When the calcination temperature is further increased, the PXRD diagram is very similar to those previously reported for a MgAl–CO_3 hydrotalcite calcined at these temperatures, where the interlayer volatile anion has been removed [38], and only broad, low intense peaks are recorded at 2 and 1.48 Å, due to diffraction by planes (2 0 0) and (2 2 0), respectively, of periclase, MgO.

The FTIR spectrum of the sample calcined at 200 °C is very similar to that of the uncalcined sample; however, upon calcination at 300 °C no band is recorded which could be ascribed to the intercalated drug, further confirming that decomposition takes place between 200 and 300 °C; the weak bands recorded at 1632, 1480, and 1379 cm^{-1}, recorded in the spectrum of the sample calcined above 400 °C, are probably due to water and CO_2 adsorbed on the external surface of the crystallites; it should be taken into account that the large specific surface area of the sample calcined at this temperature makes very easy the absorption of these gases, and that samples were exposed to air after calcination and prior to recording the FTIR spectra.

The TG and DTA for the hydrotalcite–naproxen samples were very similar for both samples, and those for NapC are included in Fig. 5. A weak endothermic effect is recorded at ca. 100 °C, probably associated to removal of interlayer water molecules, followed by an extremely intense exothermic effect, due to combustion of the organic anion. A second exothermic effect at 321 °C is also recorded. Contrary to sample SalC, a continuous weight loss is recorded in this case, which is not completed even at 1000 °C. The behavior observed for these samples upon calcination at increasing temperatures is very similar to that of the MgAl–salicylate samples. The PXRD diagrams are amorphous for the samples calcined at 300 °C and higher temperatures, indicating that the layered structure is destroyed between 200 and 300 °C; the FTIR bands of the naproxen molecule also disappear at 300 °C, and the only crystalline species detected in the calcined samples is MgO.

4. Discussion

The results reported indicate that the two methods used here are appropriated to intercalate these two drug molecules into the interlayer space of hydrotalcite.

In the case of salicylic acid, Mg_2Al–salicylate LDHs have been obtained, with a small carbonate and bicarbonate contamination. These anions should be located in the interlayer, together with the salicylate anion, in order to balance the positive charge of the layers, arising from the Mg^{2+}/Al^{3+} substitution, because the Al/salicylate ratio is larger than one. The absence of diffraction lines of phases containing these anions in the PXRD diagrams suggests that these species are highly dispersed, forming mostly an amorphous phase.

The results are very similar for naproxen samples, although in this case bicarbonate was not detected in any case and carbonate contamination is not observed by any technique for sample NapC, where a small amount of chloride, which is not removed upon washing, is detected.

The presence of carbonate in most of the samples does not allow the determination of definitive formulae for the samples prepared. Only for sample NapC, which is not contaminated by carbonate, the following formula can be proposed:

$$[Mg_{0.67}Al_{0.33}(OH)_2]\,(Naproxen)_{0.26}\,Cl_{0.07}\cdot m\,H_2O$$

Both from a chemical or a pharmacological point of view, both routes are adequate to intercalate these drugs in the interlayer of hydrotalcite, as carbonate and bicarbonate are not toxic and the small contamination by chloride is extremely low to be harmful.

The height of the gallery in the sample Mg_2Al–salicylate prepared, once the thickness of the brucite-like layers (4.8 Å [10]) has been substracted, was 11.5 Å. This value is very close to those previously reported (10.4–10.7 Å) by other authors [12,14–16] for intercalation of benzoate, which molecular dimensions are very similar to those of salicylate, or in systems obtained upon intercalation of salicylate in Zn,Cr or Zn,Al hydrotalcites [12]. The values for the NapR and NapC samples were 16.6 and 15.8 Å, respectively.

Non-spherical anions can be located in different orientations in the interlayer space; one of the factors determining this orientation is the area of layer per unit charge, and the area of the anion itself. In our case, the areas are 28.7 and 65 $Å^2$/charge for salicylate and naproxen, respectively, as concluded from the dimensions of the molecules, Fig. 6, determined using the CS Chem 3D Pro programme. The area of the layers corresponding to a charge unit is close to 24 $Å^2$/charge, as calculated using the formula $a^2\sqrt{3}/2\xi$, where $a = 2\,d_{110}$ and ξ is the positive charge of the layer (i.e., x) [12]. The area available depends on the Mg/Al ratio: the larger the Al content, the larger the positive charge of the layers and lower the area per charge unit. Consequently, we should not expect these drugs will locate with their molecular plane parallel to the brucite-like layers, but upwards or somewhat tilted.

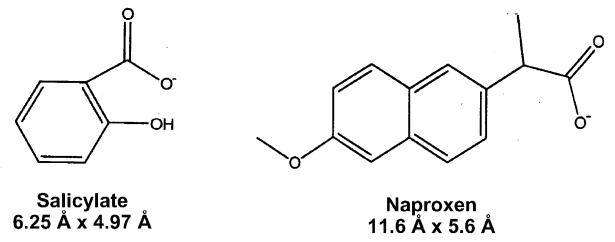

Fig. 6. Molecular dimensions of the free drugs, as determined with the CS Chem 3D Pro programme.

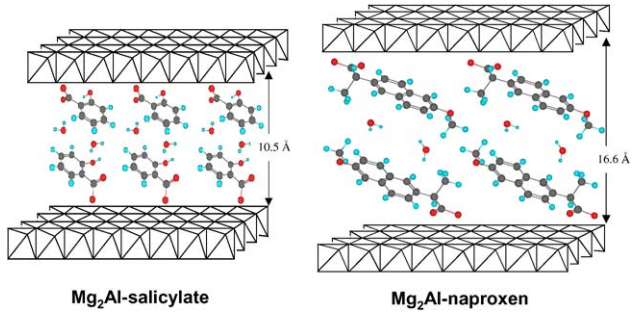

Fig. 7. Sketches of the possible location of salicylate and naproxen in the interlayer space of the MgAl hydrotalcites.

Jones et al. [14] have incorporated benzoate in MgAl hydrotalcites in two different fashions: perpendicular to the layers, forming a bilayer (when Mg/Al = 2), or parallel to the layers forming a monolayer (with Mg/Al > 2). The reasons for these different orientations are the charge of the layers, the temperature, and the hydration degree of the sample. In our case, we did not succeed in incorporating salicylate in LDHs with Mg/Al > 2, and in the case of naproxen the solids are poorly crystallized and are noticeably contaminated.

The largest dimension of the drug molecule, taking into account the dimensions of the molecules and the van der Walls radii of the "external" atoms, is 9 Å for salicylate and 13 Å for naproxen. These values are markedly smaller than the gallery height experimentally measured for our samples, and thus even a completely perpendicular orientation would not account for the experimental results. Thus, formation of bilayers should be assumed.

Carlino and Hudson [39] have reported that location of monocarboxylate anions in the interlayer of hydrotalcites is more difficult than that of dicarboxylates: In this last case both negative ends would interact with the brucite-like layers, while in the former case such an interaction would proceed only through one of the ends of the organic molecule, and the molecules would be free to form bilayers with different orientation.

Several orientations have been proposed for intercalation of benzoate, an anion with molecular dimensions close to those of salicylate. The anion forms a bilayer with the carboxylate groups pointing towards the hydroxide layers and the aromatic ring are in the middle of the gallery [16,40]; other authors [12] have proposed a vertical orientation of the benzoate molecule, with a water molecule between the aromatic ring and the hydroxide layers. NEXAFS studies by Moggridge et al. [41] indicate a bilayer orientation, but the benzoate molecules are tilted, forming an angle of $35 \pm 10^{\circ}$ with the hydroxyl layers.

Takagi et al. [42] have studied incorporation of monocarboxylate anions, such as *p*-phenyl cinnamate and stilbenecarboxylate, finding a gallery height equal or slightly larger, respectively, than the dimensions of the hosted anions; they assume an anti-parallel packing of the molecules, the carboxylate groups of two consecutive molecules pointing to alternate brucite-like layers. Ogawa and Asai [43] have used the coprecipitation method to prepare MgAl–deoxycholate hydrotalcites with Mg/Al molar ratios ranging from 2 to 20; from the gallery height measured, the hosted anion should form a tilted bilayer, with electrostatic interactions between the carboxylate groups and the layers. As the Mg/Al ratio increases the basal spacing decreases because of a different orientation of the molecules with the decrease in the positive charge of the layers. A similar tilted bilayer packing is proposed by Fardella et al. [28,29] for a MgAl–dichlofenac prepared by anion exchange of a MgAl–Cl hydrotalcite.

Although the experimental techniques here used do not permit a conclusive determination of the orientation of the anions in the interlayer, according to the PXRD data recorded and the literature information above summarized, we can propose the orientation depicted in Fig. 7, i.e., a tilted bilayer with the carboxylate groups pointing toward the brucite-like layers.

The study carried out on the evolution of the samples with the calcination temperature indicates that all systems are stable up to 230 °C; above this temperature, decomposition and combustion of the anion takes place, collapsing the layered structure, with simultaneous dehydroxylation of the layer, forming amorphous Mg and Al oxides. The behavior observed for higher calcination temperatures is similar to that reported in the literature for MgAl–CO_3 hydrotalcites. The solids prepared by calcination display a very large specific surface area, specially for the hydrotalcite–naproxen system.

Acknowledgments

Finantial support from Junta de Castilla y León (Consejería de Educación y Cultura, grant SA101/01).

References

[1] W.T. Reichle, Solid State Ion. 22 (1986) 135.
[2] K.A. Corrado, A. Kostapapas, S.L. Suib, Solid State Ion. 26 (1988) 77.
[3] F. Cavani, F. Trifiró, A. Vaccari, Catal. Today 11 (1991) 1.
[4] A. de Roy, C. Forano, K. El Malki, J.P. Besse, Synthesis of microporous materials, in: M.L. Occelli, H.E. Robson (Eds.), Expanded Clays and Other Microporous Solids, vol. II, Van Nostrand Reinhold, New York, 1992, p. 108.
[5] F. Trifiró, A. Vaccari, in: J.L. Atwood, J.E.D. Davis, D.D. MacNicol, F. Vogtle, J.M. Lehn, G. Alberti, T. Bein (Eds.), Comprehensive Supramolecular Chemistry, vol. 7, Pergamon–Elsevier Sci. Ltd., Oxford, 1996, p. 251.
[6] S.P. Newman, W. Jones, New J. Chem. 22 (1998) 105.
[7] V. Rives, M.A. Ulibarri, Coord. Chem. Rev. 181 (1999) 61.
[8] V. Rives (Ed.), Layered Double Hydroxides: Present and Future, Nova Sci. Pub., Inc., New York, 2001.
[9] S. Carlino, Solid State Ion. 98 (1997) 73.
[10] M.A. Drezdzon, Inorg. Chem. 27 (1988) 4628.
[11] P.K. Dutta, M. Puri, J. Phys. Chem. 93 (1989) 376.
[12] M. Meyn, K. Beneke, G. Lagaly, Inorg. Chem. 29 (1990) 5201.
[13] M.R. Weir, J. Moore, R.A. Kydd, Chem. Mater. 9 (1997) 1686.
[14] F. Kooli, I.C. Chisem, M. Vucelic, W. Jones, Chem. Mater. 8 (1996) 1969.
[15] M. Vucelic, G.D. Moggridge, W. Jones, J. Phys. Chem. 99 (1995) 8328.
[16] W. Kagunya, M. Chibwe, W. Jones, Mol. Cryst. Liq. Cryst. 24 (1994) 155.
[17] T. Sato, A. Okuwaki, Solid State Ion. 45 (1991) 43.
[18] W. Kagunya, J. Phys. Chem. 100 (1996) 327.
[19] T. Makino, S. Marunaka, S. Imoto, Eur. Patent E P, 638, 313, 1993, to Takeda Chemical Industries, Ltd., C.A. vol. 122 (1995) 170248s.
[20] C. Fritsch, H. G. Wetzstein, A.-G. Bayer, German Patent 3,612,086, 1986; CA 108 (1988) 173550f.
[21] P. Grubel, D.R. Cave, Aliment Pharmacol. Ther. 12 (1998) 569.
[22] A. Ooukobo, K. Ooi, H. Hayashi, J. Pharm. Sci. 81 (1992) 1139.
[23] J. S. Woo, H. G. Yi, US Patent 99, 411,510, 2000 to Hanmi Pharm. Co., Ltd; C.A. 132 (2000) 227449.
[24] Y.W. Chien, Novel Drug Delivery Systems: Fundamental, Development Concepts, Biomedical Assessments, second ed, Marcel Dekker, New York, 1991.
[25] N. Doi, S. Nitta, M. Kusakari, N. Takahashi, Jpn. Kokai Tokkyo Koho JP 60,225,719 [85,225,719], 1984; C.A. 104 (1986) 155998w.
[26] K. Watanabe, Y. Sato, N. Kikuchi, Jpn. Kokai Tokkyo Koho JP 98,101,907, 1999; C.A. 131 (1999) 303377.
[27] M. Nocchetti, Chimica dell′intercallazione in Argille Anionichi Sintetiche e in Fosfati Lamellari, Tesi di Dottorato in Scienze Chimiche, Universita degli Studi di Perugia, Italy, 1998.
[28] G. Fardella, L. Perioli, V. Ambrogi, G. Grandolini, U. Constantino, M. Nochetti, Proc. Int. Symp. Controlled Release Bioact. Mater. 24 (1997) 1033.
[29] G. Fardella, L. Perioli, G. Grandolini, Proceedings of the 25th International Symposium on Controlled Release of Bioactive Materials vol. 25 (1998) 774.
[30] V. Ambrogi, G. Fardella, G. Grandolini, M. Nocchetti, L. Perioli, J. Pharm. Sci. 92 (2003) 1407.
[31] F. Burriel, F. Lucena, S. Arribas, J. Hernández, Química Analítica Cuantitativa, thirteenth ed, Paraninfo, Madrid, 1989.
[32] W.T. Reichle, S.Y. Kang, D.S. Everhardt, J. Catal. 101 (1986) 352.
[33] V. Rives, in: V. Rives (Ed.), Layered Double Hydroxides: Present and Future, Nova Sci. Pub., Inc., New York, 2001, p. 229 (Chapter 8).
[34] V.A. Drits, A.S. Bookin, in: V. Rives (Ed.), Layered Double Hydroxides: Present and Future, Nova Sci. Pub., Inc., New York, 2001, p. 39 (Chapter 2).
[35] L.J. Bellamy, The Infrared Spectra of Complex Molecules, Chapman & Hall, London, 1975.
[36] J.T. Kloprogge, R.L. Frost, in: V. Rives (Ed.), Layered Double Hydroxides: Present and Future, Nova Sci. Pub., Inc., New York, 2001, p. 139 (Chapter 5).
[37] S. Carlino, M.J. Hudson, J. Mater. Chem. 4 (1994) 99.
[38] F.M. Labajos, V. Rives, M.A. Ulibarri, J. Mater. Sci. 27 (1992) 1546.
[39] S. Carlino, M.J. Hudson, J. Mater. Chem. 5 (1995) 1433.
[40] M. Vucelic, Ph. D. Thesis, University of Cambridge, 1995.
[41] G.D. Moggridge, G. Tourillon, Clays Clay Miner. 42 (1994) 462.
[42] K. Takagi, T. Shichi, H. Usami, Y. Sawaki, J. Am. Chem. Soc. 115 (1993) 4339.
[43] M. Ogawa, S.H. Asai, Chem. Mater. 12 (2000) 3253.